



Microencapsulation of pomegranate (*Punica granatum* L.) seed oil by complex coacervation: Development of a potential functional ingredient for food application[☆]

André M.M. Costa^a, Leticia K. Moretti^a, Grazieli Simões^b, Kelly A. Silva^c, Verônica Calado^d,
Renata V. Tonon^{e,*}, Alexandre G. Torres^{a,1}

^a Laboratório de Bioquímica Nutricional e de Alimentos, Instituto de Química, Universidade Federal do Rio de Janeiro, Rio de Janeiro, Brazil

^b Departamento de Físico-Química, Instituto de Química, Universidade Federal do Rio de Janeiro, Rio de Janeiro, Brazil

^c Departamento de Bromatologia (MBO), Universidade Federal Fluminense, Rio de Janeiro, Brazil

^d Escola de Química, Universidade Federal do Rio de Janeiro, Rio de Janeiro, Brazil

^e Embrapa Agroindústria de Alimentos, Rio de Janeiro, Brazil

ARTICLE INFO

Keywords:

Pomegranate seed oil
Punicic acid
Complex coacervation
Whey protein
Gum Arabic

ABSTRACT

The objective of this study was to develop a functional ingredient containing punicic acid, a bioactive conjugated linolenic acid isomer, via microencapsulation of pomegranate seed oil (PSO) by complex coacervation. Whey protein and gum Arabic were used as encapsulating agents and spray drying was applied as a hardening step. The effects of total polymer concentration (C_p) (2.2–7.8 g/100 mL) and wall material:oil ratio (WM:Oil) (0.5–5.0) on microparticles physical-chemical characteristics (oil retention, microencapsulation efficiency (ME), punicic acid content and particle size) were evaluated, according to a 2² rotatable central composite design. Microparticles' morphology and surface composition were also assessed. Both C_p and WM:Oil ratio affected oil retention, ME, punicic acid content and particle size. Intermediate values of C_p and WM:Oil ratio were considered the best conditions for PSO encapsulation, resulting in the highest oil retention (near 100 g/100 g; and punicic acid content, near 64 g/100 g fatty acid). High C_p and low WM:Oil ratios promoted microparticles' agglomeration. PSO microparticles rich in punicic acid were successfully produced by complex coacervation, enabling future use of PSO as a functional ingredient in food products.

1. Introduction

Pomegranate (*Punica granatum*) is a fruit appreciated for its pulp flavor and color, being mainly destined for the production of juice, nectar, jam and jellies (Shabbir et al., 2017). The seeds represent a major pomegranate residue (3.7–7.9 g/100 g fruit weight) from juice and jelly industries, consisting of a rich source of lipids (12–20 g/100 g) with an interesting chemical composition in terms of bioactive compounds (Fernandes et al., 2015), but they are largely discarded. Pomegranate seed oil (PSO) is known for its high contents of tocopherols, phytosterols and phenolic compounds. However, the described functional activities, such as cytotoxic effect, modulation of the immune

system and anti-diabetic properties, seem to be associated with its singular fatty acid profile (Viladomiu, Hontecillas, Lu, & Bassaganya-Riera, 2013). PSO is composed chiefly by conjugated linolenic acid isomers (cLnAs), specially punicic acid, which corresponds to approximately 70 g/100 g of total fatty acids in the oil (Fernandes et al., 2015).

cLnA is a collective term for the positional and geometric isomers of linolenic acid (C18:3), characterized by the presence of three conjugated double bonds, usually in positions Δ9,11,13, and Δ8,10,12 and with varying combinations of geometrical configurations, *cis* or *trans* (Cao, Gao, Chen, Chen, & Yang, 2006). Although cLnA isomers are emerging as potential bioactive nutrients, studies in humans evaluating

[☆] Chemical compounds studied in this article: <-eleostearic acid (PubChem CID: 5281115); *-eleostearic acid (PubChem CID: 5282820); catalpic acid (PubChem CID: 5385589); punicic acid (PubChem CID: 5281126).

* Corresponding author. Embrapa Agroindústria de Alimentos., Av. das Américas, 29501- Guaratiba, CEP 23020-470, Rio de Janeiro, RJ, Brazil.

E-mail addresses: andreme_1@hotmail.com (A.M.M. Costa), leticia_korin@hotmail.com (L.K. Moretti), grazielisimoes@iq.ufrj.br (G. Simões), kalenkar@yahoo.com.br (K.A. Silva), calado@eq.ufrj.br (V. Calado), renata.tonon@embrapa.br, renata.tonon@embrapa.br (R.V. Tonon), torres@iq.ufrj.br (A.G. Torres).

¹ These authors share senior authorship.

Table 1

Oil retention, microencapsulation efficiency (ME), punicic acid content, moisture, water activity (a_w), particle size, for the 11 trials of the experimental design. (Mean \pm SD).

F	C_p (g/100 mL)	Ratio (WM:Oil)	Oil retention (g/100 g)	ME (g/100 g)	Punicic acid content (g/100 g fatty acid)	Moisture content (g/ 100 g)	a_w	Particle size	
								D[0.5] (μ m)	Span
1	3 (-1)	1.15 (-1)	78.05 \pm 3.23	50.00 \pm 0.88	60.48 \pm 0.54	3.81 \pm 0.28	0.410 \pm 0.011	8.43 \pm 0.24	3.33 \pm 0.08
2	3 (-1)	4.35 (+1)	75.00 \pm 0.01	55.16 \pm 0.11	60.49 \pm 0.74	4.81 \pm 0.28	0.329 \pm 0.002	9.18 \pm 1.53	2.24 \pm 0.59
3	7 (+1)	1.15 (-1)	98.58 \pm 1.06	43.17 \pm 4.17	60.69 \pm 1.83	1.91 \pm 0.42	0.353 \pm 0.001	10.08 \pm 0.51	1.27 \pm 0.17
4	7 (+1)	4.35 (+1)	88.64 \pm 4.68	60.76 \pm 2.09	59.95 \pm 0.37	4.21 \pm 0.01	0.288 \pm 0.006	8.67 \pm 0.25	1.29 \pm 0.05
5	2.17 (-1.41)	2.75 (0)	60.33 \pm 2.71	61.40 \pm 0.84	59.88 \pm 0.78	5.30 \pm 0.41	0.366 \pm 0.006	8.36 \pm 1.38	3.75 \pm 0.12
6	7.82 (+1.41)	2.75 (0)	85.08 \pm 1.11	62.92 \pm 0.18	61.22 \pm 0.19	3.21 \pm 0.28	0.219 \pm 0.006	10.96 \pm 0.75	1.61 \pm 0.21
7	5 (0)	0.48 (-1.41)	106.19 \pm 0.44	38.52 \pm 1.92	62.12 \pm 0.38	0.4 \pm 0.28	0.285 \pm 0.036	9.10 \pm 0.10	1.53 \pm 0.07
8	5 (0)	5.01 (+1.41)	83.23 \pm 3.43	67.40 \pm 5.31	61.08 \pm 1.71	4.19 \pm 0.34	0.230 \pm 0.006	8.82 \pm 0.44	0.99 \pm 0.06
9 ^a	5 (0)	2.75 (0)	95.2 \pm 0.08	55.46 \pm 4.62	62.93 \pm 2.14	4.92 \pm 0.71	0.283 \pm 0.001	9.29 \pm 0.09	1.54 \pm 0.24
9 ^a	5 (0)	2.75 (0)	94.28 \pm 3.04	56.98 \pm 0.59	64.22 \pm 0.5	4.19 \pm 0.52	0.379 \pm 0.004	10.28 \pm 0.12	1.41 \pm 0.29
9 ^a	5 (0)	2.75 (0)	105.41 \pm 0.13	48.74 \pm 0.47	63.85 \pm 1.1	4.38 \pm 0.28	0.331 \pm 0.068	10.13 \pm 1.08	1.92 \pm 0.06

F: Formulation; ^acentral point; C_p : polymer concentration in the emulsion; WM: wall material a_w : water activity; D[0.5]: maximum size (μ m) of 50% analyzed particles; span: particle size scattering index.

the health benefits of its acute or chronic consumption are still scarce, because these compounds, especially punicic acid, are restricted to PSO and *Trichosanthes kirilowii* seed oil (Shabbir et al., 2017). The development of food products using PSO as a functional ingredient could stimulate its consumption and help to clarify the oil bioactivity. However, direct addition of PSO aiming at supplementing food products is limited by its hydrophobic nature and by the high susceptibility of cLnA isomers to lipid oxidation when exposed to oxygen and light (Yang, Cao, Chen, & Chen, 2009). Thus, these functional lipids should be protected in order to preserve their physical and chemical stability, avoiding oxidative rancidity and nutritional losses.

Microencapsulation is a "packing" technique in which an active ingredient is covered by a wall material, being often used to protect unstable molecules from the interaction with other components and the adjacent environment during food processing and storage (Gouin, 2004).

Complex coacervation is an encapsulation method that consists of a liquid-liquid phase separation phenomenon that occurs when electrostatically opposite charged biopolymers are subjected to specific conditions, producing aggregates (coacervates) that promptly deposit on the oil droplets. Compared to other encapsulation techniques, complex coacervation is able to produce microparticles with higher microencapsulation efficiency, using high core load and low wall material concentration (Gouin, 2004). The process performance and the physicochemical properties of particles produced by complex coacervation can be influenced by parameters such as: total polymers concentration, protein:polysaccharide ratio, core:wall material ratio, pH, salt concentration and others (Weinbreck, de Vries, Schrooyen, & de Kruijff, 2003). For established complex coacervate systems, such as whey protein:gum Arabic and gelatin:gum Arabic, some factors (protein:polysaccharide ratio, pH and salt concentration) are well known (Weinbreck et al., 2003; Weinbreck, Tromp, & de Kruijff, 2004), while other parameters need to be studied in order to provide satisfactory process performance, when new core nutrients are used. Whey protein-gum Arabic system has been successfully used to encapsulate a wide range of hydrophobic materials (Eratte et al., 2015; Eratte, Wang, Dowling, Barrow, & Adhikari, 2014; Weinbreck, Minorf, & Kruijff, 2004). Nevertheless, to the best of our knowledge, microencapsulation of PSO by complex coacervation using this system has not yet been studied.

This work aimed at investigating complex coacervation as a suitable method for microencapsulation of pomegranate seed oil, using whey protein and gum Arabic as encapsulating system. The effect of total polymer concentration (C_p) and wall material:oil ratio (WM:Oil ratio) on the dried microparticles properties was assessed, according to a

rotatable central composite design, aiming to define the best micro-particle formulation. Oil retention, microencapsulation efficiency, punicic acid content and particle size were analyzed as responses. Microparticles morphology and surface composition were also evaluated.

2. Material and methods

2.1. Materials

Cold-pressed commercial pomegranate seed oil (PSO) (C16:0 = 2.25 g/100 g, C18:0 = 1.86 g/100 g, C18:1n-9 = 4.52 g/100 g, C18:1n-7 = 0.41 g/100 g, C18:2n-6 = 5.29 g/100 g, C20:0 = 0.61 g/100 g, C20:1 n-9 = 0.78 g/100 g, Total cLnA = 84.3 g/100 g) (Oneva Food Co[®], Istanbul, Turkey) was used as core material. Whey protein isolate (WPI) (Alibra[®], São Paulo, Brazil) and Gum Arabic (GA) (Instantgum BA[®], Colloides Naturels, São Paulo, Brazil) were used as wall materials for particles production.

A commercial mixture of fatty acid methyl esters (37-component FAME mix; Supelco, Bellefonte, PA, US) and individual cLnA isomers (punicic acid, alpha-eleostearic acid, catalpic acid and beta-eleostearic acid; Larodan AB, Solna, Sweden) were used as standards for fatty acid identification in gas-chromatographic analyzes. All solvents used were HPLC grade from Tedia (São Paulo, Brazil) and all reagents used were from Merck (Darmstadt, Germany).

2.2. Production of the PSO's microparticles by complex coacervation

PSO's microparticles were produced as follows: firstly, the wall materials (WPI and GA) were separately weighed and dissolved in distilled water under magnetic stirring during 30 min, at room temperature, to obtain the solutions with C_p values described in Table 1. The solutions' pH was adjusted to 7.0 with HCl (0.5 mol/L) and NaOH (0.5 mol/L), and the WPI:GA ratio was 2:1 (Weinbreck et al., 2004). After dissolution, PSO was added dropwise to the WPI solution under continuous stirring (16,000 rpm) during 5 min with an Ultra-Turrax homogenizer (T25-IKA[®], IKA, Wilmington, US), to produce a stable emulsion. Then, GA solution was mixed with the previous emulsion and homogenized for 1 min at 16,000 rpm. Finally, emulsion's pH was adjusted to 3.75 by adding HCl (1.0 mol/L) (Eratte et al., 2014) aiming at inducing electrostatic interactions between WPI and GA, thus forming the wet microparticles. Microencapsulation process was carried out at 25 °C, for 10 min.

A rotatable central composite design was applied to evaluate the effect of total polymer concentration (C_p) (2.2–7.8 g/100 mL) and wall

material:oil ratio (WM:Oil ratio) (0.5–5.0) on the microencapsulation of PSO by complex coacervation, according to Table 1.

The following polynomial equation was fitted to data (Equation (1)):

$$y = \beta_0 + \beta_1x_1 + \beta_2x_2 + \beta_{11}x_1^2 + \beta_{22}x_2^2 + \beta_{12}x_1x_2 \quad (1)$$

where β_n are constant regression coefficients, y is the response for dried particles physicochemical properties (oil retention, microencapsulation efficiency, punicic acid content, moisture content, water activity or particle size), and x_1 and x_2 are the coded independent variables (C_p and WM:Oil ratio).

2.3. Drying of the PSO's microparticles

Immediately after preparation, the wet microparticles were dried in a laboratory scale spray dryer (SD-06AG, Lab Plant, North Yorkshire, UK) equipped with a 0.5 mm nozzle. The drying conditions were: inlet air temperature of 180 °C, outlet air temperature of 66 ± 4 °C, air flow pressure of 2.5×10^5 Pa and feed flow rate of 0.5 L/h. Dried microparticles were collected, sealed in plastic bags under vacuum, covered in aluminum foil and stored at -80 °C for further characterization.

2.4. Wet microparticles morphology

Wet microparticles morphology was evaluated in an optical microscope (Eclipse E200; Nikon®, Tokyo, Japan) coupled to a digital camera (Evolution VF, Media Cybernetics, Rockville, MD, US). Prior to observation in the microscope, microparticles were collected from the formulations by centrifugation (11,739 \cdot g, 10 min) and were diluted twice with ultrapure water acidified with 0.5 mol/L HCl (pH 3.7). Images were registered at $400 \times$ and $1000 \times$ magnifications.

2.5. Dried microparticles analysis

2.5.1. Oil retention

Total oil content present in the microparticles was determined in a Soxhlet apparatus (SER 148; Velp® Scientifica, Usmate, Italy), according to Goula and Adamopoulos (2012), with few modifications. The oil extracted with petroleum ether added with BHT was weighed, re-suspended with a known volume of hexane with BHT (0.05 g/100 mL) and stored at -20 °C until further analysis.

Oil retention was defined as the percentage of total oil in the final powder to that initially added in the feed emulsion and was calculated as follows (Equation (2)):

$$\text{Oil retention (g/ 100 g)} = \frac{\text{Mass of total oil (g)}}{\text{Mass of oil in the feed emulsion (g)}} \times 100 \quad (2)$$

2.5.2. Microencapsulation efficiency (ME)

Surface oil was determined according to Sankarikutty, Sreekumar, Narayanan, and Mathew (1988), with the modifications proposed by Kouassi et al. (2012). ME was calculated according to Equation (3):

$$\text{ME (g/ 100 g)} = \frac{\text{Total oil (g)} - \text{Surface oil (g)}}{\text{Total oil (g)}} \times 100 \quad (3)$$

2.5.3. Punicic acid content

PSO fatty acids extracted from the microparticles were methylated by a base-catalyzed transesterification procedure (Kramer et al., 1997) to avoid isomerization. PSOs' fatty acid methyl esters (FAME) were analyzed by gas chromatography with a flame ionization detector (GC-FID) and equipped with a split/splitless injector (GC-2010 chromatograph; Shimadzu, Japan) exactly as described by Costa, Silva, and Torres (2019). Fatty acid composition results were expressed as g/100 g

fatty acid.

2.5.4. Moisture content and water activity (a_w)

Moisture content was determined in all samples using a moisture balance with infrared radiation heating (MA35 Mettler Toledo, Urdorf, Switzerland). Water activity was assessed in a water activity analyzer (LabMaster-aw, Novasina AG, Lanchen, Switzerland).

2.5.5. Particle size

PSO microparticles were dispersed in isopropanol and analyzed in a particle size analyzer SDC-Microtrac S3500 (Microtrac, Montgomeryville, PA, US) by the scattering pattern of a transverse laser light. Results were reported as $D[0.5]$ and scattering index (*Span*) (Equation (4)), which are defined as the mean diameter (μm) and width distribution of particles size range, respectively.

$$\text{Span} = \frac{D[0.9] - D[0.1]}{D[0.5]} \quad (4)$$

where: $D[0.9]$, $D[0.1]$ and $D[0.5]$ are the diameters at 10, 50, and 90% cumulative volume, respectively.

2.5.6. Morphology

PSO microparticles' morphology was evaluated by scanning electron microscopy (SEM). Samples were directly deposited on carbon conductive tape on aluminum SEM stubs, and coated with a thin gold layer, using a gold-sputter (Desk V, Denton Vacuum®, Moorestown, NJ, US). The samples were analyzed using a Tescan Vega 3 SEM (Tescan®, Kohoutovice, Czech Republic) operated at 15 kV.

2.5.7. X-ray photoelectron spectroscopy (XPS) of microparticles

XPS analysis was performed on a UHV Xi ESCALAB 250 (Thermo Fisher Scientifics, US) spectrometer equipped with a hemispherical electron energy analyzer. The XPS spectra were collected using monochromatic Al K α X-ray source (1486.6 eV) and an electron emission angle of 90° with the surface. Survey scans were recorded with 1 eV steps and 100 eV analyzer pass energy. The high-resolution C1s spectra were recorded with 0.1 eV steps and 25 eV pass energy analyzer. The linearity of the energy scale was checked using Cu (932.7 eV), Ag (368.3 eV) and Au (84.0 eV) lines. Data processing was performed using Thermo Avantage software. Peak fitting was carried out with Lorentzian/Gaussian ratio of 30%/70%.

2.6. Statistical analysis

For the central composite design, analysis of variance (ANOVA), test of lack of fit, determination of regression coefficients and the construction of response surface (3D) graphs, Statistica 7.0 (StatSoft, Tulsa, US) software was used. Statistical comparisons were based on at least triplicate results, and all data were presented as mean and standard deviation. The influence of the encapsulation process on cLnA isomer distribution was evaluated by comparing a mean obtained from the distribution of each cLnA isomers from the 11 formulations tested, with a non-encapsulated sample, using *t*-test. Data were analyzed with GraphPad Prism v.6.0 (GraphPad software 2012, La Jolla, CA, US), and the bar graphs displayed in this work were also plotted using this program. Significance level was established at $p < 0.05$.

3. Results and discussion

3.1. Morphology of wet microparticles

A noticeable coacervate layer around the oil droplets was noticeable in most of the formulations (Fig. 1), indicating the effectiveness of the encapsulation process. Formulations with higher oil content showed larger oil droplets (Fig. 1a, c and 1g), which can suggest that coalescence may be starting after homogenization ceased, indicating that

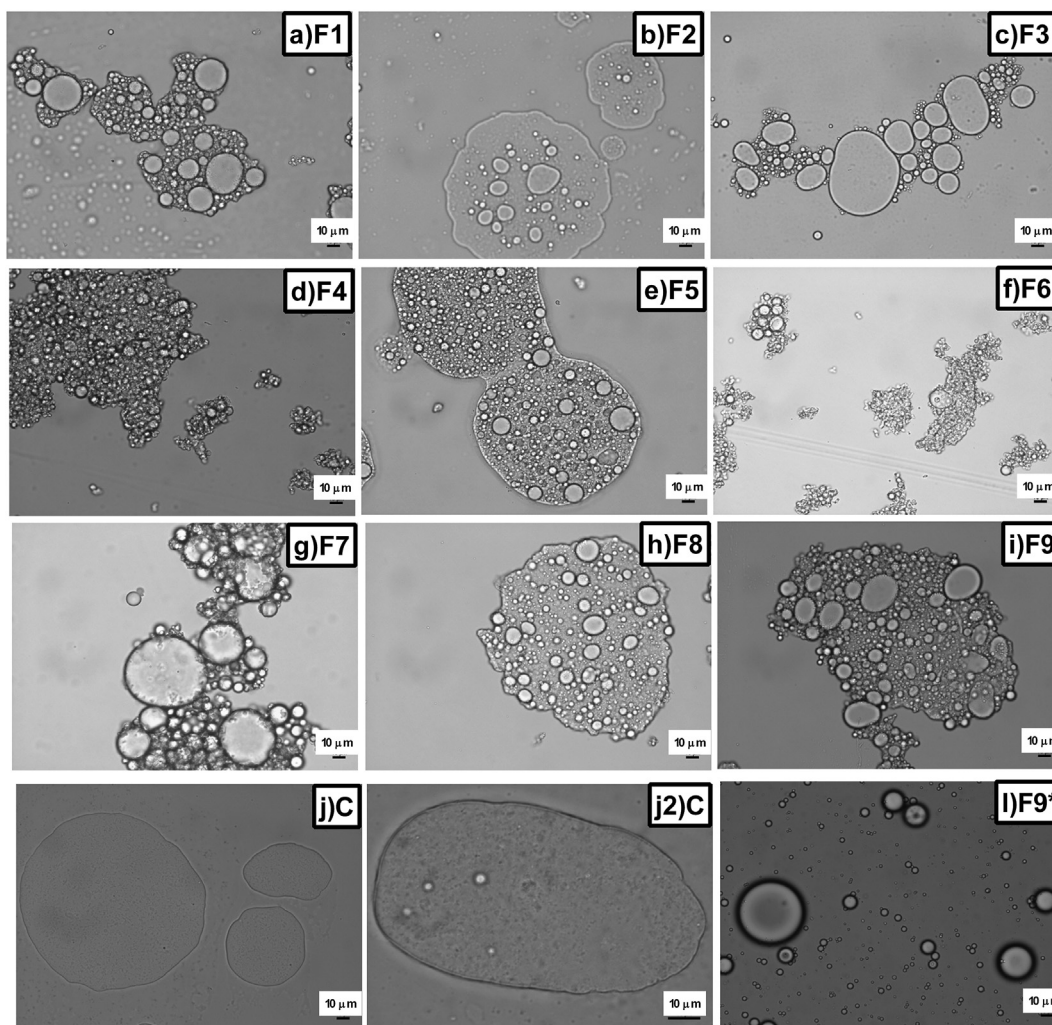


Fig. 1. Wet capsules' micrographs of the experimental design formulations obtained by optical microscopy: a) 1, C_p : 3 g/100 mL; WM:Oil: 1.15; b) 2, C_p : 3 g/100 mL; WM:Oil: 4.35; c) 3, C_p : 7 g/100 mL; WM:Oil: 1.15; d) 4, C_p : 7 g/100 mL; WM:Oil: 1.15; e) 5, C_p : 2.17 g/100 mL; WM:Oil: 2.75; f) 6, C_p : 7.82 g/100 mL; WM:Oil: 2.75; g) 7, C_p : 5 g/100 mL; WM:Oil: 0.48; h) 8, C_p : 5 g/100 mL; WM:Oil: 5.01; i) 9, C_p : 5 g/100 mL; WM:Oil: 2.75; j) Coacervate (C); j2) Coacervate (C); l) Formulation 9 produced at pH 7. Wet capsules were prepared in pH 3.7, whey protein: gum Arabic ratio (2:1) and reaction time of 10 min a, b, c, d, e, f, g, h, i, j and m: magnification of $400\times$; j2: magnification of $1000\times$.

these structures were less stable than the other formulations. Formulation 9 was used as a negative control at pH = 7.0, in which WPI and gum Arabic have similar net charges and thus suppressing coacervation. As expected, there was no coacervate layer adsorbed on the oil droplets in this formulation (Fig. 1l). The coacervates without PSO showed a transparent gel-like structure (Fig. 1j and 1j2) (Weinbrecht et al., 2004). All formulations showed multi-cored microparticles (Fig. 1), which generally occurs when high homogenization rates are used during the emulsification step prior to coacervation (Eratte et al., 2014; Kaushik, Dowling, McKnight, Barrow, & Adhikari, 2016; Liu, Low, & Nickerson, 2010).

Polymer concentration did not show a clear effect on particles morphology, while the WM:Oil ratio influenced the coacervate layer thickness. When comparing formulations with the same polymer concentration and distinct WM:Oil ratios (F1 vs. F2; F3 vs. F4; F7 vs. F8 vs. F9; Fig. 1a vs 1b; Fig. 1c vs 1d and Fig. 1g vs 1h vs 1i), it is possible to notice that an increase in the WM:Oil ratio resulted in a thicker coacervate layer. This same trend was also observed by Ma, Zhao, Wang, and Sun (2019), using the same technology to encapsulate methyl oleate applying gelatin:Gum Arabic system. According to Goula and Adamopoulos (2012), microparticles with a thicker coacervate layer are more suitable to the atomization process, because a minimum length

between the core and microcapsule's surface should be kept in order to avoid oil droplets migration to particles' external layer, thus reducing microparticles surface oil.

3.2. Dried microparticles

PSO's microparticles moisture content and a_w varied from 0.4 to 5.3 g/100 g and 0.219–0.410, respectively, which are values commonly observed in microparticles produced by spray drying (moisture ≤ 6 g/100 g and $a_w \leq 0.6$) (Klaypradit & Huang, 2008; Reineccius, 2004).

3.2.1. Experimental design

The results for each response analyzed in the central composite design are shown in Table 1. The regression coefficients for the polynomial equation, F values and determination coefficients (R^2) for each response are shown in Table 2. The calculated F values were higher than the tabulated ones for all the evaluated responses, except for ME, indicating that this response could not be predicted by the adjusted model.

3.2.1.1. Oil retention. The presence of unbound oil on the dryer wall was only observed in formulation 7, which had the highest oil content

Table 2

Coded second-order regression coefficients, *F* values and determination coefficients (*R*²) for oil yield, microencapsulation efficiency (ME), punicic acid content and particle size scattering index (Span).

Coefficient	Oil retention (g/100 g)	ME (g/100 g)	Punicic acid content (g/100 g fatty acid)	Span
β_0	98.29**	53.75**	63.67**	1.62**
β_1	8.66*	0.12	0.19	-0.76**
β_{11}	-12.51**	2.90	-1.73**	0.55**
β_2	-5.69	7.96*	-0.27	-0.23
β_{22}	-1.44	-1.73	-1.21*	-0.17
β_{12}	-1.72	3.11	-0.19	0.28
<i>F</i> _{calculated}	13.91	4.6	8.4	57.98
<i>F</i> _{tabulated}	5.05	5.05	5.05	5.05
<i>R</i> ²	0.932	0.821	0.896	0.980

β_0 : mean; β_1 : Total polymer concentration linear; β_{11} : Total polymer concentration quadratic; β_2 : Wall material: oil (WM:Oil) ratio linear; β_{22} : WM:Oil ratio quadratic; β_{12} : Total polymer concentration \times WM:Oil ratio. *significant at *p* < 0.06; **significant at *p* < 0.05.

(lowest WM:Oil ratio) and showed the lowest oil retention (60.3 \pm 2.71 g/100 g), while all other formulations showed oil retention between 75 and 106 g/100 g. These values were sensibly

higher than those previously observed in the microencapsulation of flaxseed and tuna oil by complex coacervation (Eratte et al., 2014; Kaushik et al., 2016; Liu et al., 2010). Oil retention was positively influenced by *C_p* (Table 2), until a maximum *C_p* value ranging from 5 to 7 g/100 mL (Fig. 2a). Previous studies suggested that the increase of *C_p* implies in an increase of emulsion viscosity (Frascareli, Silva, Tonon, & Hubinger, 2011; Goula & Adamopoulos, 2012; Sahin-Nadeem & Özen, 2014). Viscosity of the coacervate layer is important to form a resistant barrier around the oil droplet, thus favoring oil retention during the drying process.

3.2.1.2. Microencapsulation efficiency. Microencapsulation efficiency (ME) varied from 38.5 g/100 g–67.4 g/100 g (Table 1) and was positively influenced by the WM:Oil ratio (Table 2), thus formulations with WM:Oil ratios equal to or higher than 2.75 showed the highest values of ME (Table 1). For this variable, a response surface was not presented, due to the lack of fit of the proposed model (*R*² = 0.82 and *F*_{calculated} < *F*_{tabulated}) (Table 2).

The influence of WM:Oil ratio on ME observed in this study has also been described in previous works (Jun-xia, Hai-yan, & Jian, 2011; Kaushik et al., 2016; Yang, Gao, Hu, Li, & Sun, 2015). Similarly to the oil retention, this result could be associated to the higher proportions of oil droplets close to the drying surface, which shortens the diffusion

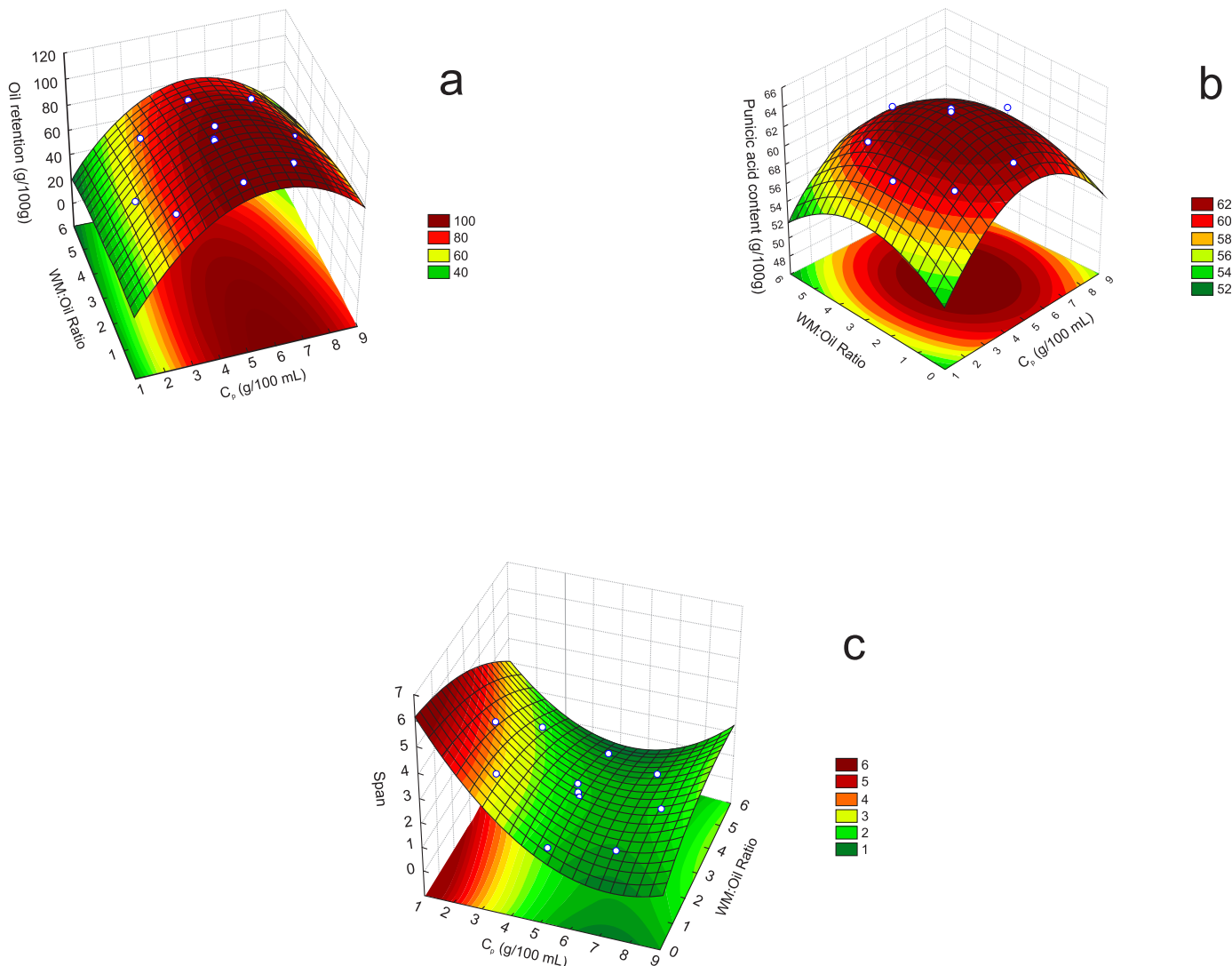


Fig. 2. Response surfaces of: a) oil yield; b) punicic acid content; and c) *Span*. **C_p*: Total polymer concentration, WM = wall material.

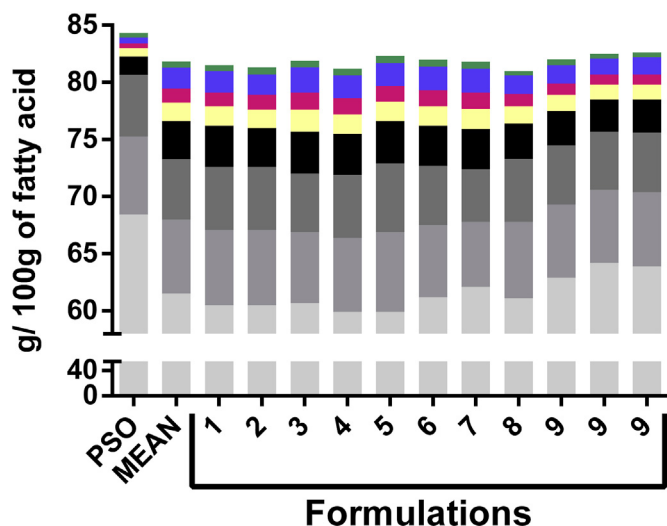


Fig. 3. Fatty acid composition in pomegranate seed oil and in microparticles produced with different formulations. The encapsulation process influenced all cLnA isomers distribution (t -test, $p < 0.05$). *■: cLnA 4; ■: cLnA 3; ■: cLnA 2; ■: cLnA 1; ■: Beta-eleostearic acid; ■: Catalpic acid; ■: Alfa-eleostearic acid; ■: Punicic acid.

path length to the drying microcapsule external layer. Wet microparticles' micrographs in Fig. 1 agree with this trend, as it is possible to notice that WM:Oil ratio influenced the coacervate layer thickness. Additionally, at low WM:Oil ratios (high oil loads), the C_p could have not been enough to completely cover the oil droplets and prevent oil droplets coalescence. Consequently, large droplets were surrounded by a thin coacervate layer, while small droplets were encapsulated by a matrix of coacervate, as shown in Fig. 1.

3.2.1.3. Punicic acid retention in microparticles. PSO is a rich source of a family of bioactive fatty acids, namely cLnA (Fig. 3). GC analysis showed eight cLnA isomers, from which four (punicic, alpha-eleostearic, catalpic and beta-eleostearic acids) were identified based on comparisons with standards' retention times and mass spectrometric fragmentation profiles (Supplementary Fig. 1; Costa et al., 2019). Punicic acid is the major cLnA in PSO and its content is associated to the oil's functional properties (Viladomiu et al., 2013). Being PSO highly oxidizable because of its high cLnA content, the encapsulation process promoted a small but significant loss of punicic acid (Fig. 3), possibly by oxidation. In parallel, beta-eleostearic acid and other minor cLnA isomers (cLnA 1, cLnA 2, cLnA 3 and cLnA 4; Supplementary Fig. 1) contents increased from 1.5- to 3.6-fold, indicating that part of punicic acid was isomerized, probably because of the high temperatures applied in the drying process (Sahin-Nadeem & Afşin Özen, 2014) and because the *trans*-isomers are more stable than the *cis*-isomers of cLnA (Giua, Blasi, Simonetti, & Cossignani, 2013).

Punicic acid content varied only slightly among the PSO microparticles formulations (from 59.9 to 64.2 g/100 g oil, Table 1). However, these marginal differences might result in a final product with sensibly different punicic acid content, as microparticles' oil load varied up to 4-fold among formulations, for instance, 5.01 WM:Oil ratio had 16.6 g PSO/100 g of microparticles vs. 0.48 WM:Oil ratio that had 67.7 g PSO/100 g of microparticles. The response surface graph shows a region of maximum punicic acid content on the intermediate levels of C_p and WM:Oil ratio (Fig. 2b). ME values were positively associated to punicic contents, consequently, having low amounts of non-encapsulated punicic acid on the particle surface might delay PSO oxidation.

3.2.1.4. Particle size. PSO microparticles showed a small variation in the mean diameter (8.36–10.96 μ m), with no significant influence of

any independent variable, and an overall narrow particle size distribution, demonstrated by the low *Span* values (Table 1).

According to the experimental design results, only C_p significantly affected the *Span* value of PSO's microparticles (Table 2), and low *span* values were found in microparticles with C_p between 5 and 7.82 g/100 mL (Fig. 2c). Particles with narrow particle size distribution are appealing for food application, as this characteristic is considered important to promote a sustained core release (Walton & Mumford, 1999).

As the coacervates were not crosslinked, microparticles' structure could have been partially broken during atomization. Thus, it is possible that the particles' diameters observed refer to particle fragments, and not to their original structure. This hypothesis could be evaluated by comparing crosslinked and non-crosslinked structures after atomization.

3.2.1.5. Dried PSO microparticles' morphology. Surface morphology of the PSO microparticles is shown in Fig. 4. Most of the formulations showed spherical shape and variable sizes with numerous invaginations, which is typical of spray-dried microparticles (Ré, 1998). Similar morphology was observed by Eratte et al. (2015; 2014) and Rutz et al. (2017), which also microencapsulated edible oils by complex coacervation and used spray drying as a hardening/recovery step. However, as mentioned, the original structure of the non-crosslinked coacervates could have been broken during atomization, resulting in a new arrange of polymer material with the same morphology of traditional spray-dried particles. Thus, we cannot rule out that the particles observed in Fig. 4 are in fact not the original coacervates.

In the formulations with a WM:Oil ratio of 2.75 (Fig. 3e, f and 3i), the increase of C_p above 5 g/100 mL promoted noticeable aggregation problems (Fig. 4). This phenomenon could be associated to an overbalance of the wall materials, which intensified microparticles adhesion, due to an increase in the feed emulsion viscosity (Yang et al., 2015). Regarding oil load, formulations with a WM:Oil ratio of 1.15 or lower also showed aggregation problems. These problems were more evident in Formulation 7 (Fig. 4g), where microparticles' structure collapsed, and it was not possible to observe surface features of individual microparticles. This could be attributed to the high surface oil content present in these formulations, which may have enhanced microparticles stickiness (Goula & Adamopoulos, 2012). Interesting morphological characteristics for food application were demonstrated in WM:Oil ratios between 2.75 and 4.35, such as spherical shape microparticles with minimal structure break.

3.3. Selection of the best formulation

The variables used to select the best formulation were oil retention, ME and punicic acid content. Based on these responses, the intermediate values of C_p and WM:Oil ratio ($C_p = 5$ g/100 mL, WM:Oil ratio = 2.75) were chosen. Although this formulation did not show the highest values of ME, it was located in the region near the optimal values of oil retention and punicic acid content (Fig. 2a and b), showing the highest content of the featured bioactive compound in PSO and a considerable load of PSO per gram of dried microparticles (26.6 g PSO/100 g microparticles).

3.4. XPS analysis

The concentration of different carbon species was determined by curve fitting the high-resolution C1s spectra. The spectra of the WM (coacervate without oil), WPI, GA, the elected formulation (F9) and F7 (formulation with the lowest ME: 38.5 g/100 g) showed carbon components with the following assignments: C1 (C–C, C–H); C2 (C–O, C–N); C3 (C=O, O–C–O, N–C=O) and C4 (O–C=O). The C1s high resolution spectra are shown in Fig. 5b, c, 5d, 5e and 5f. The XPS analysis of oil was impractical in ultra-high vacuum as it is liquid.

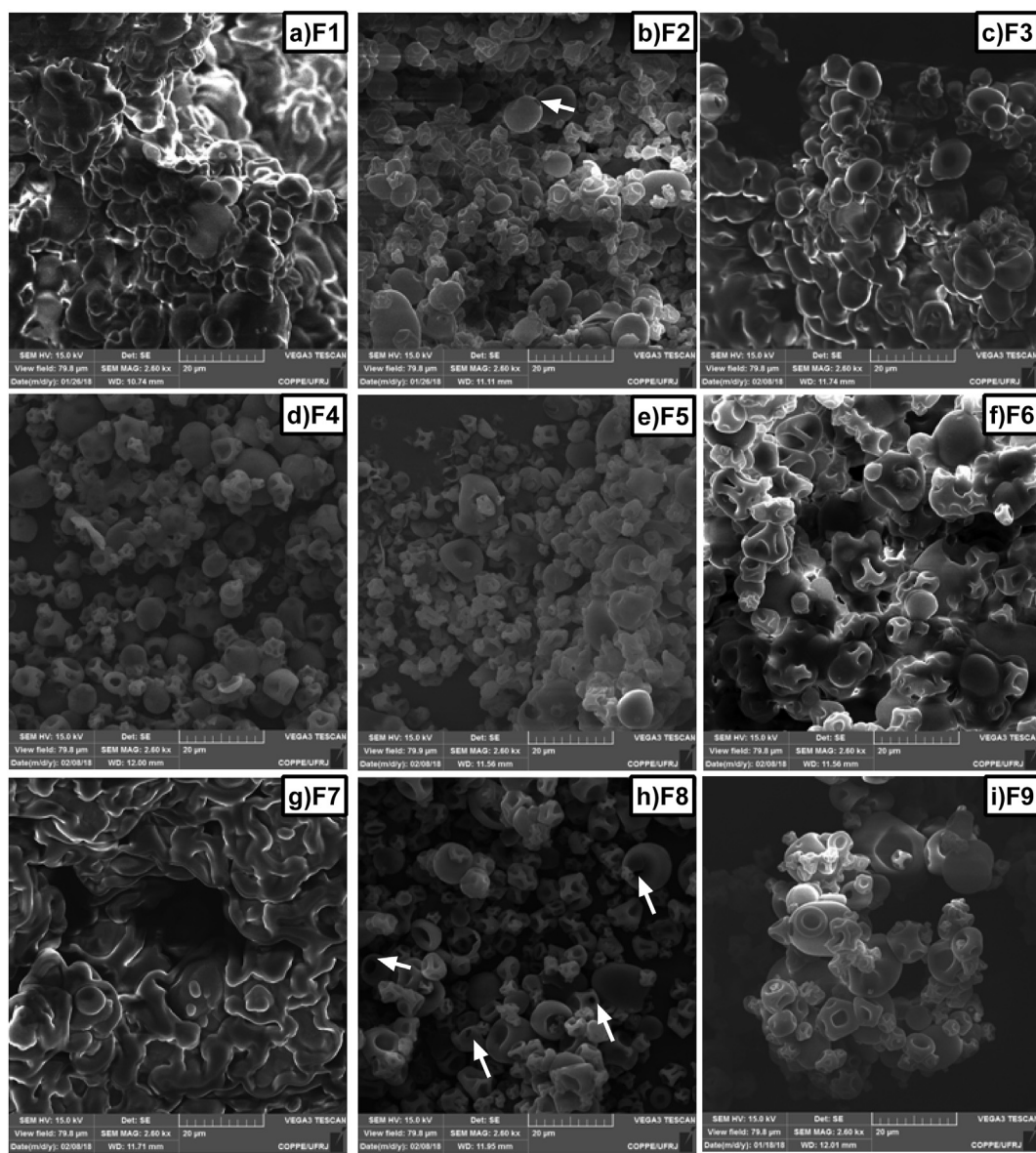


Fig. 4. Dried microparticles micrographs of the experimental design formulations obtained by scanning electron microscopy (SEM): a) 1, C_p : 3 g/100 mL; WM:Oil: 1.15; b) 2, C_p : 3 g/100 mL; WM:Oil: 4.35; c) 3, C_p : 7 g/100 mL; WM:Oil: 1.15; d) 4, C_p : 7 g/100 mL; WM:Oil: 1.15; e) 5, C_p : 2.17 g/100 mL; WM:Oil: 2.75; f) 6, C_p : 7.82 g/100 mL; WM:Oil: 2.75; g) 7, C_p : 5 g/100 mL; WM:Oil: 0.48; h) 8, C_p : 5 g/100 mL; WM:Oil: 5.01; i) 9, C_p : 5 g/100 mL; WM:Oil: 2.75. Bar = 20 μ m. White arrows indicate cracks and open pores.

The C1s spectrum of WPI is characterized by a particularly strong C1 contribution (Fig. 5c). This characteristic is not expected for a protein spectrum but can result from the presence of lipids on the surface. The GA peaks (Fig. 5d) showed, as expected, a typical polysaccharide spectrum, dominated by the C–O peak. This was confirmed in the survey spectrum by a strong oxygen signal and very little or no nitrogen signal (Fig. 5a). Surface composition of coacervate WM presented characteristics of both WPI and GA (Fig. 5b). F9 and F7 spectra combine characteristics of WPI spectrum, such as prominent C1 chemical environment (Fig. 5e and f) and the presence of nitrogen in the survey spectra (Fig. 5a), indicating that different concentrations of C_p and WM:Oil ratio results in variations in microparticles surface composition. XPS analysis was tentatively used to evaluate microparticles surface composition, because this method does not modify samples' surface composition, as the classical washing methods applied earlier. Therefore, after evaluating the C1–4 chemical environment, a relation between the O=C=O peak was observed, highlighted as acid/ester groups, and a higher content of surface oil, as samples with

encapsulated PSO showed higher contributions of C4 than the control with no PSO (WPI, GA, WM; Table 3). This result could also be extrapolated to all formulations (Fig. 6), because C4 peak intensity was negatively influenced by ME results (Table 1), indicating agreement between XPS results and the washing method described earlier. Jafari, Assadpoor, Bhandari, and He (2008) microencapsulated fish oil by spray drying and also observed an agreement between both methods. Additionally, XPS analysis was also capable to indicate interactions between WPI and GA, as the C3 and C4 chemical environment increased in WM, F9 and F7 (Table 3), probably because a higher exposure of WPI (NH_3^+) and GA (COO^-) interaction sites on microparticles surface, resulting from pH adjustment (Eratte et al., 2015).

4. Conclusion

PSO was successfully microencapsulated by complex coacervation, showing a minimal impact on PSO isomer distribution. The feed emulsion formulation had a significant influence on the coacervation

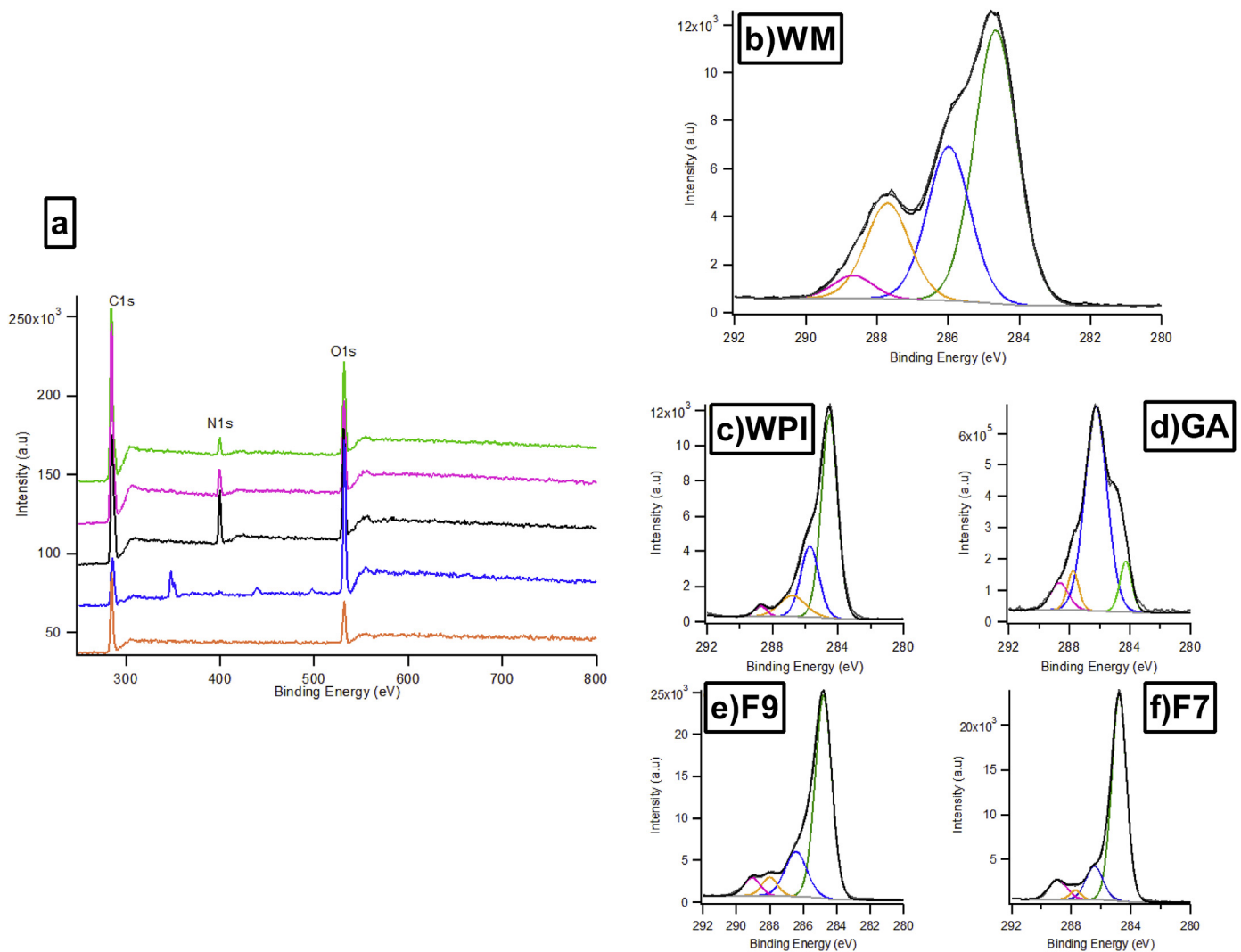


Fig. 5. Microparticles' X-ray photoelectron spectroscopy (XPS) analysis. a) XPS survey spectra of wall material (WM), whey protein isolate (WPI), gum Arabic (GA), elected formulation (F9: C_p: 5 g/100 mL; WM:Oil: 2.75), and formulation with the lowest microencapsulation efficiency (F7: C_p: 5 g/100 mL WM:Oil: 0.48); and XPS C1s high-resolution spectra of b) WM, c) WPI, d) GA, e) F9, f) F7.

*C1 (C–C, C–H); C2 (C–O, C–N); C3 (C=O, O–C–O, N–C=O) and C4 (O–C=O). a) ■ F7; ■ F9; ■ WM; ■ GA; ■ WPI. In b), c), d), e) and f), ■ C1s data; ■ C1; ■ C2; ■ C3; ■ C4; ■ background; ■ fit.

Table 3

Surface elemental composition of formulations (F9: C_p: 5 g/100 mL; WM:Oil: 2.75 and F7: C_p: 5 g/100 mL; WM:Oil: 0.48) and components (WM, GA, WPI), determined by X-ray photoelectron spectroscopy (XPS).

Elemental Composition	WM (%)	GA (%)	WPI (%)	F9 (%)	F7 (%)
C1 (C–C, C–H)	52.1	16.4	74.3	71.7	74.3
C2 (C–O, C–N)	21.9	77.3	19.2	19.0	16.5
C3 (C=O, O–C–O, N–C=O)	22.6	4.5	4.6	5.0	0.4
C4 (O–C=O)	3.4	1.8	1.9	4.3	8.8

process and microparticles physical-chemical and morphological properties. Among the physical-chemical properties evaluated in this study, oil retention, ME, punnic acid content and *Span* values were influenced by experimental design factors. Moreover, surface analysis determined by XPS was accurate, being especially indicated for porous wall systems aiming at avoiding extraction of the encapsulated oil. Microparticles produced with 5 g/100 g of C_p and WM:Oil ratio of 2.75 were selected as the most promising ones, due to the highest punnic acid content and oil retention. In the present study, coacervation

process parameters manipulation enabled the design of PSO's microparticles with physical-chemical properties that allows its application in food products. However, it remains to be confirmed if the original coacervates' structure was kept during spray drying, since the high pressure and turbulent flow inside the atomizer could have broken the particles structure without altering the gross morphology of the obtained powder.

CRediT authorship contribution statement

André M.M. Costa: Conceptualization, Methodology, Formal analysis, Investigation, Data curation, Writing - original draft, Visualization, Project administration. **Leticia K. Moretti:** Investigation, Visualization. **Grazieli Simões:** Methodology, Formal analysis, Investigation, Visualization, Writing - original draft. **Kelly A. Silva:** Methodology, Formal analysis, Investigation, Visualization, Writing - original draft. **Verônica Calado:** Methodology, Formal analysis. **Renata V. Tonon:** Conceptualization, Methodology, Resources, Data curation, Writing - review & editing, Supervision, Funding acquisition. **Alexandre G. Torres:** Conceptualization, Methodology, Resources, Data curation, Writing - review & editing, Supervision, Funding

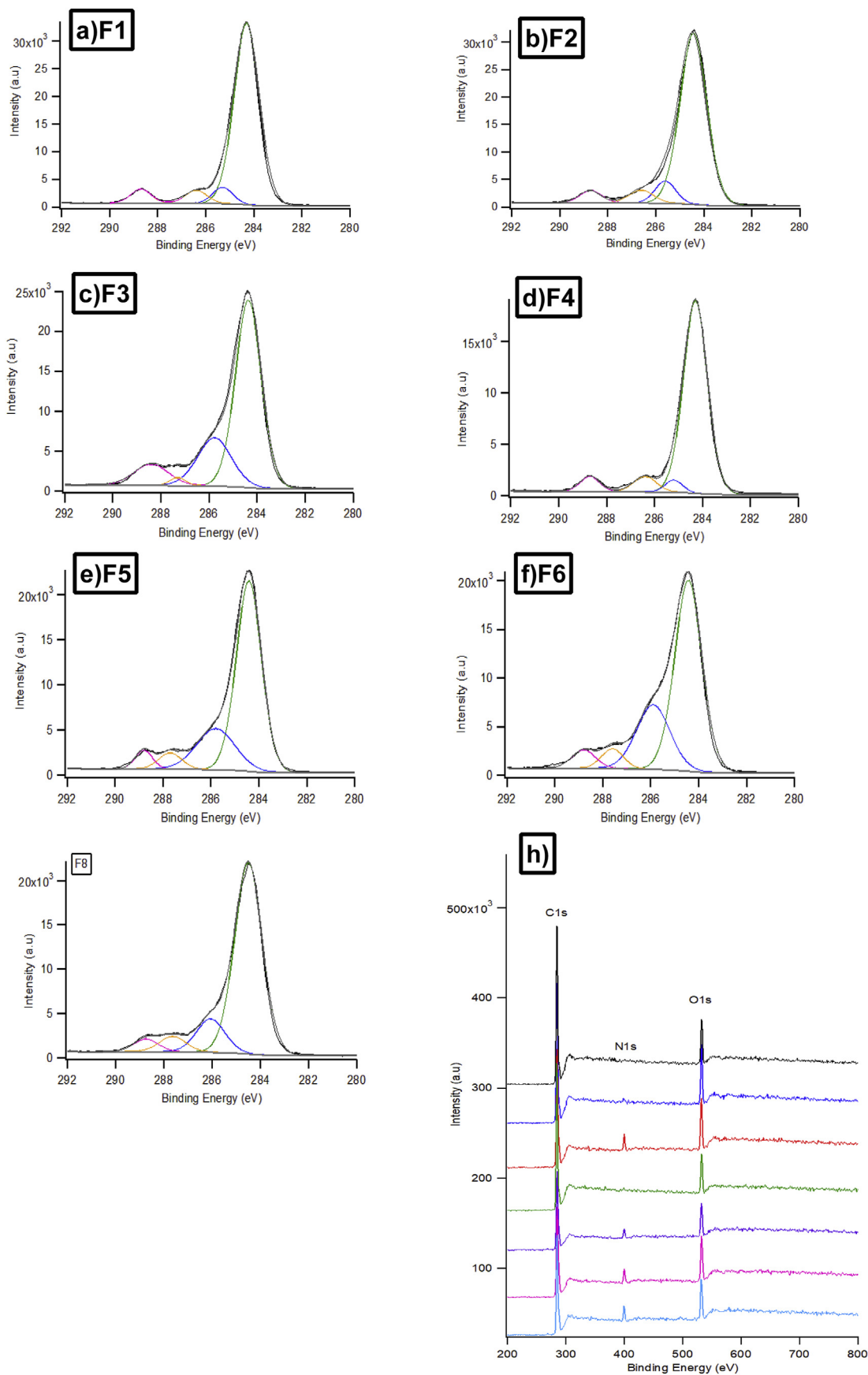


Fig. 6. Microparticles' X-ray photoelectron spectroscopy (XPS) analysis. XPS C1s high-resolution spectra of Formulations: a) 1, C_p: 3 g/100 mL; WM:Oil: 1.15; b) 2, C_p: 3 g/100 mL; WM:Oil: 4.35; c) 3, C_p: 7 g/100 mL; WM:Oil: 1.15; d) 4, C_p: 7 g/100 mL; WM:Oil: 1.15; e) 5, C_p: 2.17 g/100 mL; WM:Oil: 2.75; f) 6, C_p: 7.82 g/100 mL; WM:Oil: 2.75; g) 8, C_p: 5 g/100 mL; WM:Oil: 5.01) and h) XPS survey spectra of Formulations 1, 2, 3, 4, 5, 6 and 8.

*In a), b), c), d), e), f) and g), ■: C1s data; ■: C1; ■: C2; ■: C3; ■: C4; ■: background; ■: fit; and in h) ■: F1; ■: F2; ■: F3; ■: F4; ■: F5; ■: F6; ■: F8.

acquisition.

Declaration of competing interest

The authors declare that there are no conflicts of interest.

Acknowledgements

This work was supported by CAPES (Finance code 001), CNPq (grants number 432484/2016-7, 309558/2015-8 and 310659/2018-3) and FAPERJ (grant numbers E-26/010.001277/2015, E-26/203.197/2015 and E-26/203.294/2016) (Brazil). AGT and RVT are recipients of CNPq and FAPERJ scholarships, AMMC was a recipient of a CNPq PhD studentship. We are also grateful to Brenda Duarte Galraha for assistance in some of the laboratory analysis.

Appendix A Supplementary data

Supplementary data to this article can be found online at <https://doi.org/10.1016/j.lwt.2020.109519>.

References

- Cao, Y., Gao, H. L., Chen, J. N., Chen, Z. Y., & Yang, L. (2006). Identification and characterization of conjugated linolenic acid isomers by Ag⁺-HPLC and NMR. *Journal of Agricultural and Food Chemistry*, *54*, 9004–9009.
- Costa, A. M. M., Silva, L. O., & Torres, A. G. (2019). Chemical composition of commercial cold-pressed pomegranate (*Punica granatum*) seed oil from Turkey and Israel, and the use of bioactive compounds for samples' origin preliminary discrimination. *Journal of Food Composition and Analysis*, *75*, 8–16.
- Eratte, D., McKnight, S., Gengenbach, T. R., Dowling, K., Barrow, C. J., & Adhikari, B. P. (2015). Co-encapsulation and characterisation of omega-3 fatty acids and probiotic bacteria in whey protein isolate-gum Arabic complex coacervates. *Journal of Functional Foods*, *19*, 882–892.
- Eratte, D., Wang, B., Dowling, K., Barrow, C. J., & Adhikari, B. P. (2014). Complex coacervation with whey protein isolate and gum Arabic for the microencapsulation of omega-3 rich tuna oil. *Food Funct.* *5*, 2743–2750.
- Fernandes, L., Pereira, J. A., López-Cortés, I., Salazar, D. M., Ramalhosa, E., & Casal, S. (2015). Fatty acid, vitamin E and sterols composition of seed oils from nine different pomegranate (*Punica granatum* L.) cultivars grown in Spain. *Journal of Food Composition and Analysis*, *39*, 13–22.
- Frascarelli, E. C., Silva, V. M., Tonon, R. V., & Hubinger, M. D. (2011). Food and Bioproducts Processing Effect of process conditions on the microencapsulation of coffee oil by spray drying. *Food and Bioproducts Processing*, *90*, 413–424.
- Giua, L., Blasi, F., Simonetti, M. S., & Cossignani, L. (2013). Oxidative modifications of conjugated and unconjugated linoleic acid during heating. *Food Chemistry*, *140*(4), 680–685.
- Gouin, S. (2004). Microencapsulation: Industrial appraisal of existing technologies and trends. *Trends in Food Science & Technology*, *15*, 330–347.
- Goula, A. M., & Adamopoulos, K. G. (2012). A method for pomegranate seed application in food industries: Seed oil encapsulation. *Food and Bioproducts Processing*, *90*, 639–652.
- I Ré, M. (1998). Microencapsulation by spray drying. *Drying Technology*, *16*, 1195–1236.
- Jafari, S. M., Assadpoor, E., Bhandari, B., & He, Y. (2008). Nano-particle encapsulation of fish oil by spray drying. *Food Research International*, *41*, 172–183.
- Jun-xia, X., Hai-yan, Y., & Jian, Y. (2011). Microencapsulation of sweet orange oil by complex coacervation with soybean protein isolate/gum Arabic. *Food Chemistry*, *125*, 1267–1272.
- Kaushik, P., Dowling, K., McKnight, S., Barrow, C. J., & Adhikari, B. (2016). Microencapsulation of flaxseed oil in flaxseed protein and flaxseed gum complex coacervates. *Food Research International*, *86*, 1–8.
- Klaypradit, W., & Huang, Y. W. (2008). Fish oil encapsulation with chitosan using ultrasonic atomizer. *LWT - Food Science and Technology*, *41*(6), 1133–1139.
- Kouassi, G. K., Teriveedhi, V. K., Milby, C. L., Ahmad, T., Boley, M. S., Gowda, N. M., et al. (2012). Nano-microencapsulation and controlled release of linoleic acid in biopolymer matrices: Effects of the physical state, water activity, and quercetin on oxidative stability. *Journal of Encapsulation and Adsorption Sciences*, *2*, 1–10.
- Kramer, J. G., Fellner, V., Dugan, M. R., Sauer, F., Mossoba, M., & Yurawecz, M. (1997). Evaluating acid and base catalysts in the methylation of milk and rumen fatty acids with special emphasis on conjugated dienes and total trans fatty acids. *Lipids*, *32*, 1219–1228.
- Liu, S., Low, N. H., & Nickerson, M. T. (2010). Entrapment of flaxseed oil within gelatin-gum Arabic capsules. *JAOCs. Journal of the American Oil Chemists' Society*, *87*, 809–815.
- Ma, T., Zhao, H., Wang, J., & Sun, B. (2019). Effect of processing conditions on the morphology and oxidative stability of lipid microcapsules during complex coacervation. *Food Hydrocolloids*, *87*, 637–643.
- Reineccius, G. A. (2004). The spray drying of food flavors. *Drying Technology*, *22*(6), 1289–1324 In press.
- Rutz, J. K., Borges, C. D., Zambiasi, R. C., Crizel-Cardozo, M. M., Kuck, L. S., & Noreña, C. P. Z. (2017). Microencapsulation of palm oil by complex coacervation for application in food systems. *Food Chemistry*, *220*, 59–66.
- Sahin-Nadeem, H., & Özen, M. A. (2014). Physical properties and fatty acid composition of pomegranate seed oil microcapsules prepared by using starch derivatives/whey protein blends. *European Journal of Lipid Science and Technology*, *116*, 847–856.
- Sankarikutty, B., Sreekumar, M. M., Narayanan, C. S., & Mathew, A. G. (1988). Studies on microencapsulation of cardamom oil by spray drying technique. *Journal of Food Science & Technology*, *25*, 325–355.
- Shabbir, M. A., Khan, M. R., Saeed, M., Pasha, I., Khalil, A. A., & Siraj, N. (2017). Punicic acid: A striking health substance to combat metabolic syndromes in humans. *Lipids in Health and Disease*, *16*, 1–9.
- Viladomiu, M., Hontecillas, R., Lu, P., & Bassaganya-Riera, J. (2013). Preventive and prophylactic mechanisms of action of pomegranate bioactive constituents. *Evidence-based Complementary and Alternative Medicine*, *2013*.
- Walton, D., & Mumford, C. (1999). The morphology of spray-dried particles: The effect of process variables upon the morphology of spray-dried particles. *Chemical Engineering Research and Design*, *77*, 442–460.
- Weinbreck, F., de Vries, R., Schrooyen, P., & de Kruijff, C. G. (2003). Complex coacervation of whey proteins and gum Arabic. *Biomacromolecules*, *4*, 293–303.
- Weinbreck, F., Minor, M., & Kruijff, C. G. (2004). Microencapsulation of oils using whey protein/gum Arabic coacervates. *Journal of Microencapsulation*, *21*, 667–679.
- Weinbreck, F., Tromp, R. H., de Kruijff, & De Kruijff, C. G. (2004). Composition and structure of whey protein/gum Arabic coacervates. *Biomacromolecules*, *5*, 1437–1445.
- Yang, L., Cao, Y., Chen, J. N., & Chen, Z. Y. (2009). Oxidative stability of conjugated linolenic acids. *Journal of Agricultural and Food Chemistry*, *57*, 4212–4217.
- Yang, X., Gao, N., Hu, L., Li, J., & Sun, Y. (2015). Development and evaluation of novel microcapsules containing poppy-seed oil using complex coacervation. *Journal of Food Engineering*, *161*, 87–93.